

Carbamazepine solubility in supercritical CO₂: a comprehensive study

Kalikin N.N.^{a,*}, Kurskaya M.V.^a, Ivlev D.V.^a, Krestyaninov M.A.^a, Oparin R.D.^a,
Kolesnikov A.L.^{c,*}, Budkov Y.A.^{a,b,*}, Idrissi A.^d, Kiselev M.G.^{a,*}

^a*G.A. Krestov Institute of Solution Chemistry of the Russian Academy of Sciences, Laboratory of NMR Spectroscopy and Numerical Investigations of Liquids, Akademicheskaya str. 1, 153045, Ivanovo, Russia*

^b*Tikhonov Moscow Institute of Electronics and Mathematics, School of Applied Mathematics, National Research University Higher School of Economics, 34, Tallinskaya Ulitsa, 123458, Moscow, Russia*

^c*Institut für Nichtklassische Chemie e.V., Permoserstr. 15, 04318, Leipzig, Germany*

^d*University of Lille, Faculty of Science and Technology, LASIR (UMR CNRS A8516), Bât. C5, Cité Scientifique, 59655 Villeneuve d'Ascq Cedex, France*

Abstract

In this paper we present our study of carbamazepine solubility in supercritical carbon dioxide. We have calculated the solubility values along two isochores corresponding to the CO₂ densities $\rho = 1.1\rho_{cr}(\text{CO}_2)$ and $\rho = 1.3\rho_{cr}(\text{CO}_2)$, where $\rho_{cr}(\text{CO}_2)$ is the critical density of CO₂, in the temperature range from 313 to 383 K, as well as along three isotherms at $T = 318, 328$ and 348 K by an approach based on the classical density functional theory. The solubility values were also obtained using *in situ* IR spectroscopy and molecular dynamics simulations along the mentioned isochores and isotherms, respectively. Because the density functional theory only takes into account the Lennard-Jones interactions, it can be expected to underestimate the solubility values when compared to the experimental ones. However, we have shown that the data calculated within the classical density functional theory qualitatively reproduce the solubility trends obtained by IR spectroscopy and molecular dynamics simulation. Moreover, the obtained position of the upper crossover pressure is in good agreement with the experimental literature results.

Keywords: classical density functional theory; molecular dynamics simulation; infrared spectroscopy; quantum chemical calculations; solubility; carbamazepine

1. Introduction

Nowadays a large part of the drugs presented on the pharmaceutical market are classified as Class II, according to the Biopharmaceutics Classification System (BCS) [1, 2, 3], i.e.

*Corresponding author

Email addresses: nikolaikalikin@gmail.com (Kalikin N.N.), r.d.oparin@yandex.ru (Oparin R.D.), kolesnikov@inc.uni-leipzig.de (Kolesnikov A.L.), ybudkov@hse.ru (Budkov Y.A.), mgk@isc-ras.ru (Kiselev M.G.)

demonstrate high intestinal permeability and low aqueous solubility. Such characteristics can become the reason for refusing from the production of a potentially efficient active pharmaceutical ingredient (API) during its development phase.

A number of approaches have been developed to deal with the poor drug solubility and/or dissolution issues, and at the same time to preserve the pharmacological effect of the compound. They include particle size reduction, formation of amorphous forms, salts, solvates or cocrystals [1, 4, 5, 6, 7]. Modern micronization techniques utilize specific properties of supercritical fluids, most frequently supercritical carbon dioxide (scCO₂) because of its favorable characteristics for process design. These approaches can be divided into three general groups, where scCO₂ acts as a solvent, as an antisolvent (co-antisolvent), and as an additive. Each group has its own advantages and disadvantages (Table 6 in [1]), and the choice of the method is highly dependent on the compound ability to dissolve in scCO₂. Thus, the knowledge of the drug compound solubility in the scCO₂ medium is highly valuable for the technological process of the development of a bioactive compound and its potential pharmaceutical applications. However, whether it is an experimental or a computational scheme, most of the conventional approaches, used to obtain information about the solubility of a given drug compound in the supercritical fluid (SCF), are time-consuming and resource-intensive. Recently [8], we have proposed a technique for computing solubility values based on the calculation of the drug molecule solvation free energy in scCO₂ within the classical density functional theory (cDFT). There we demonstrated the capability of our approach to qualitatively predict the solubility of ibuprofen in scCO₂ and the pressure values, at which we observe changes in the solubility dependence on temperature at a constant pressure value (pressure crossovers). The calculated solubility values were lower than the experimental ones. The observed discrepancies were attributed to the neglecting of the electrostatic interactions in the framework of the cDFT.

In the present paper, we would like to show the results of our study of carbamazepine (CBZ) solubility in scCO₂. CBZ is an essential anticonvulsant and antiepileptic representative [9, 10], also used in the treatment of bipolar disorders [11]. It features on the World Health Organization’s List of Essential Medicines [12] and at the same time belongs to Class II of the BCS [13], i.e. demonstrates high permeability and poor solubility in water. Although there is a fair number of papers featuring CBZ, the solubility data in scCO₂ for this compound are practically non-existent in literature (the paper, which we will refer to most is an experimental study by Yamini et al [14]). The paper is structured as follows: the second section describes the theoretical approach, in the third one we describe the MD simulation details, in the forth - our experimental measurements, and then we discuss the obtained results.

2. cDFT-based solubility estimation methodology

For the theoretical prediction of CBZ solubility we utilized the methodology discussed in depth in our recent papers [8]. Here we shortly describe it.

We use the following relation to determine the solubility [15], which is based on the

equilibrium condition between the solute's solid and solution phases:

$$y_2 \approx \frac{p^{sat}}{\rho_b k_B T} \exp(\beta \nu^s [p - p^{sat}] - \beta \Delta G_{solv}), \quad (1)$$

here ρ_b is the bulk density of scCO₂, k_B is the Boltzmann constant, T is the temperature, p is the total pressure imposed in the system, $\beta = (k_B T)^{-1}$; ν^s and p^{sat} are the molar volume and saturation pressure of the pure solute solid phase, respectively, and ΔG_{solv} is the solvation Gibbs free energy of the solute molecule in the scCO₂ medium. As is seen, one has to know the sublimation parameters of the solute and its solvation free energy to obtain the solubility values. Within our methodology, the data on the solute sublimation, i.e. the molar volume and saturation pressure values, is supposed to be taken from the experimental data available in literature, whereas the solvation free energy is computed with the aid of the cDFT.

We start the calculation of the solvation Gibbs free energy from writing down the grand thermodynamic potential for the scCO₂ fluid in the external potential field with the potential energy $V_{ext}(\mathbf{r})$:

$$\Omega[\rho(\mathbf{r})] = k_B T \int d\mathbf{r} \rho(\mathbf{r}) [\ln(\Lambda^3 \rho(\mathbf{r})) - 1] + F_{ex}[\rho(\mathbf{r})] + \int d\mathbf{r} \rho(\mathbf{r}) (V_{ext}(\mathbf{r}) - \mu), \quad (2)$$

where the first contribution is the Helmholtz free energy of the ideal gas, the second one is the excess Helmholtz free energy of the fluid, Λ is the thermal de Broglie wavelength, μ is the chemical potential of the bulk phase at the chosen state parameters.

The CO₂ particles are considered as spherically symmetric particles interacting through the effective pairwise Lennard-Jones (LJ) potential with the parameters defined as ε_{ff} and σ_{ff} and the distance of the cut-off $r_c = 5\sigma_{ff}$. The potential can be divided into two parts, corresponding to the contributions of the hard-core interactions and the attractive interactions between the molecules of the fluid, at its minimum $r_m = 2^{\frac{1}{6}}\sigma_{ff}$ according to the Weeks-Chandler-Andersen (WCA) procedure [16]. In this respect, the total excess free energy can be written as follows:

$$F_{ex}[\rho(\mathbf{r})] = F_{hs}[\rho(\mathbf{r})] + F_{att}[\rho(\mathbf{r})]. \quad (3)$$

The hard spheres' contribution (the first term in the right hand side of (3)) is determined utilizing Rosenfeld's version of the fundamental measure theory (FMT) [17] as follows:

$$F_{hs}[\rho(\mathbf{r})] = k_B T \int d\mathbf{r} \Phi(\mathbf{r}), \quad (4)$$

where $\Phi(\mathbf{r})$ is the excess free energy density (expressed in $k_B T$ units), which is the function of the weighted densities $n_\alpha(\mathbf{r}) = \int d\mathbf{r}' \rho(\mathbf{r}') \omega^{(\alpha)}(\mathbf{r} - \mathbf{r}')$, which, in their turn, are defined by the weight functions $\omega^{(\alpha)}(\mathbf{r})$. The latter characterize the geometric properties of the hard spheres. Defining expressions for them can be found in the review by R. Roth [18]. The Barker-Henderson (BH) diameter of the hard sphere is determined within the Pade approximation [19].

The attractive contribution to the excess free energy is described within the mean-field approximation:

$$F_{att}[\rho(\mathbf{r})] = \frac{1}{2} \int d\mathbf{r} \rho(\mathbf{r}) \int d\mathbf{r}' \rho(\mathbf{r}') \phi_{WCA}(\mathbf{r} - \mathbf{r}'), \quad (5)$$

where the effective WCA pair potential of attractive interactions is:

$$\phi_{WCA}(r) = \begin{cases} -\varepsilon_{ff}, & r < r_m \\ 4\varepsilon_{ff} \left[\left(\frac{\sigma_{ff}}{r} \right)^{12} - \left(\frac{\sigma_{ff}}{r} \right)^6 \right], & r_m < r < r_c. \end{cases} \quad (6)$$

The solute molecule is modeled as an external LJ potential:

$$V_{ext}(\mathbf{r}) = 4\varepsilon_{sf} \left[\left(\frac{\sigma_{sf}}{r} \right)^{12} - \left(\frac{\sigma_{sf}}{r} \right)^6 \right], \quad (7)$$

where the effective parameters of the interaction between this molecule and the molecules of the fluid are determined through the Berthelot-Lorenz mixing rules: $\sigma_{sf} = (\sigma_{ss} + \sigma_{ff})/2$ and $\varepsilon_{sf} = \sqrt{\varepsilon_{ss}\varepsilon_{ff}}$. The parameters of the interactions between the two molecules of the active compound (σ_{ss} , ε_{ss}) and two molecules of CO₂ (σ_{ff} , ε_{ff}) can be obtained by fitting the respective parameters of the liquid vapour critical point. One can find the values of the critical temperature and density for CO₂ at NIST [20]. We took the values for the CBZ critical temperature and pressure from the paper by Li et al [21]. The values of all the parameters are presented in Table 1.

Table 1: The values of the parameters used to calculate the solubility.

	value	source
ε_{ff}	218.73 <i>K</i>	this study
σ_{ff}	0.336 <i>nm</i>	this study
ε_{ss}	565.91 <i>K</i>	this study
σ_{ss}	0.718 <i>nm</i>	this study
ε_{sf}	351.83 <i>K</i>	this study
σ_{sf}	0.527 <i>nm</i>	this study
$T_{cr}(\text{CO}_2)$	304.13 <i>K</i>	[20]
$\rho_{cr}(\text{CO}_2)$	10.62 <i>mol/l</i>	[20]
$T_{cr}(\text{CBZ})$	786.83 <i>K</i>	[21]
$P_{cr}(\text{CBZ})$	25.71 <i>bar</i>	[21]
$\nu(\text{CBZ})$	0.18048 <i>m</i> ³ / <i>mol</i>	[21]
$p^{sat}(\text{CBZ})$	$\ln p^{sat} = 32.7 - 13343/T$	[22]

To obtain the density profile of the fluid, one has to take a variational derivative of the grand thermodynamic potential with respect to the density and iteratively compute the Euler-Lagrange equation:

$$\frac{\delta\Omega[\rho(\mathbf{r})]}{\delta\rho(\mathbf{r})} = 0, \quad (8)$$

which leads to the following expression for density:

$$\rho(\mathbf{r}) = \rho_b \exp \left[\frac{\mu_{ex}(\rho_b, T) - c_{fmt}^{(1)}(\mathbf{r}) - \int d\mathbf{r}' \rho(\mathbf{r}') \phi_{WCA}(\mathbf{r} - \mathbf{r}') - V_{ext}(\mathbf{r})}{k_B T} \right], \quad (9)$$

where μ_{ex} is the excess chemical potential of the bulk phase, $c_{fmt}^{(1)}(\mathbf{r}) = \delta F_{hs}[\rho(\mathbf{r})]/\delta \rho(\mathbf{r})$ is the one-particle direct correlation function of the hard-sphere system within FMT.

Finally, one can compute the solvation Gibbs free energy of the solute molecule in the scCO₂ medium as the excess grand thermodynamic potential as follows:

$$\Delta G_{solv} = \Omega[\rho(\mathbf{r})] - \Omega[\rho_b]. \quad (10)$$

Then, turning back to Eq. (1), we can obtain the solubility values after calculating the solvation free energy. The values of the sublimation pressure were obtained, using the empirical relation, presented in the work by Drozd et al [22], and the molar volume of the compound was taken from the paper by Li et al [21] (Table 1).

3. MD simulation and quantum chemical calculations

The CBZ solubility in scCO₂ was also estimated by MD simulation, through the same Eq. (1) with the same input parameters characterizing the solute sublimation and then by calculating the solvation free energy within the Bennett Acceptance Ratio (BAR) method [23]. Such choice was motivated by the fact that, as it was demonstrated [24, 25], the BAR method seems to be significantly more effective than the others, when it comes to more realistic modeling tests. Within this method one usually needs to perform a decent number of simulations, each corresponding to a certain intermediate step with its own coupling parameters λ , resulting in large computational costs [26]. Then one obtains the solvation free energy values by the summation of all such transitional stages from the full solute-solvent interaction coupling to none. We used the following pairwise potential of the interaction between the particles to compute the solvation free energy:

$$U_{ij}(\lambda_{LJ}, \lambda_C) = \lambda_{LJ} \times 4\varepsilon_{ij} \left[\left(\frac{\sigma_{ij}}{r} \right)^{12} - \left(\frac{\sigma_{ij}}{r} \right)^6 \right] + \lambda_C \times \frac{q_i q_j}{r}, \quad (11)$$

where λ_{LJ} and λ_C are, respectively, the alchemical scaling parameters of Lennard-Jones and Coulombic interactions; q_i, q_j are the atomic charges, ε_{ij} and σ_{ij} are the Lennard-Jones parameters of the solute-solvent interaction. We obtained these parameters through the Berthelot-Lorentz mixing rules: $\sigma_{ij} = (\sigma_{ii} + \sigma_{jj})/2$, $\varepsilon_{ij} = \sqrt{\varepsilon_{ii}\varepsilon_{jj}}$. The simulation was performed in the Gromacs 4.6.7 package [27]. For each computation of the solvation free energy 12 independent simulations were performed, each with its own potential energy (Eq. (11)), corresponding to a certain pair of the coupling parameters. The following set of the alchemical coefficients $\{\lambda_{LJ}, \lambda_C\}$ was chosen: $\{0.0, 0.0\}$, $\{0.2, 0.0\}$, $\{0.5, 0.0\}$, $\{1.0, 0.0\}$, $\{1.0, 0.2\}$, $\{1.0, 0.3\}$, $\{1.0, 0.4\}$, $\{1.0, 0.5\}$, $\{1.0, 0.6\}$, $\{1.0, 0.7\}$, $\{1.0, 0.8\}$, $\{1.0, 1.0\}$; here 0.0 and 1.0 denote the fully decoupled and fully coupled interactions between the solute

and solvent particles, respectively. The structure of the CBZ molecule was taken from the Automated Topology Builder (ATB) [28]. We used GROMOS 54A7 force-field [29] for intramolecular CBZ interactions and the Lennard-Jones contribution of intermolecular ones. The atomic partial charges of CBZ were developed based on the Merz-Kollman method [30, 31], using Gaussian 09 software [32] with the PBE functional and 6-311++g(2d,p) basis set. The atomic partial charges were averaged over two CBZ conformers (Fig.1, Table 2).

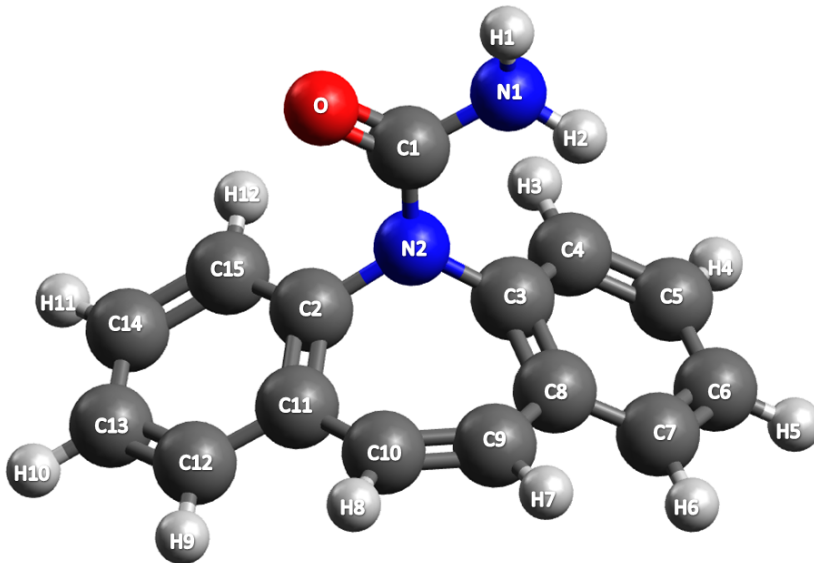


Figure 1: CBZ molecule structure.

The interaction potential for the carbon dioxide molecule corresponds to Zhang’s one [33]. The MD simulation parameters are the same as in the work by Paliwal and Shirts [34] for the case of the methane solvation free energy calculation, except for the case of the barostat choice, as we used Parinello-Rahman pressure coupling. Each simulation was performed for 100 *ps* in the NVT ensemble with a step of 1 *fs*, for 1 *ns* in the NPT ensemble with a step of 2 *fs* and for 10 *ns* of the production run simulation in the NPT ensemble with a step of 2 *fs*. We used the experimental data from Yamini’s paper [14] as the basis and computed two isotherms at 328 and 348 *K* with pressures corresponding to those presented in the paper.

4. Infrared spectroscopy experiment

We also measured experimentally the solubility of CBZ in *scCO*₂ using *in situ* infrared spectroscopy. The obtained values were compared with those obtained by MD and cDFT methods as well as with those obtained by Yamini [14].

The experimental solubility values are generally given in the form of solubility isotherms. However, in our *in situ* IR experiment, we measured the solubility along the isochores,

Table 2: Calculated partial charges.

number	atom	charge	number	atom	charge
1	H1	0.364805	16	H6	0.148109
2	N1	-0.815994	17	C8	0.276173
3	H2	0.330523	18	C9	-0.322119
4	C1	0.709618	19	H7	0.152478
5	O	-0.568671	20	C10	-0.178388
6	N2	-0.305988	21	H8	0.138673
7	C2	0.217946	22	C11	0.162796
8	C3	0.070900	23	C12	-0.217421
9	C4	-0.130436	24	H9	0.132605
10	H3	0.137536	25	C13	-0.116918
11	C5	-0.170959	26	H10	0.126729
12	H4	0.135166	27	C14	-0.129340
13	C6	-0.090339	28	H11	0.130257
14	H5	0.123977	29	C15	-0.222715
15	C7	-0.262720	30	H12	0.173718

because in the experiment we used a high pressure high temperature (HPHT) optical cell with a constant volume, as it is the case in many supercritical micronization techniques.

In order to measure the solubility (concentration of a saturated solution) of CBZ in scCO₂, we used the approach developed in our previous works [35] [36]. This approach is centered around the Beer–Lambert law and, in particular, on the usage of the integral extinction coefficient ε_{int} (molar absorption coefficient) value of a chosen analytical spectral band. For this purpose, we registered the IR spectra of CBZ, dissolved in an inert solvent that had no specific interactions with the CBZ molecules. The integral extinction coefficient was calculated by the following formula:

$$\varepsilon_{int} = \frac{A}{lc} \quad (12)$$

where l is the optical path length of the sample (cm), c is the molar concentration of the solute ($mol \cdot ml^{-1}$), A is the integral intensity (cm^{-1}). In its turn, the integral intensity is calculated as follows:

$$A = \int_{\nu_1}^{\nu_2} \log \frac{I_0(\nu)}{I(\nu)} d\nu, \quad (13)$$

where ν_1 and ν_2 are the boundaries of the analytical spectral band, I_0 and I are the incident and transmitted intensities, respectively.

Within the *in situ* IR approach, the integral extinction coefficient of the C=O vibration mode of the CBZ chosen as an analytical spectral band was calculated. This band has a good resolution and high signal-to-noise ratio within the whole studied temperature range. Then we recorded the IR spectra of the CBZ diluted in tetrahydrofuran (THF) in the temperature range of 313 – 383 K with a step of 10 K . The molar concentration of the prepared solution

was $1.1755 \cdot 10^{-2} \text{ mol} \cdot \text{l}^{-1}$, which corresponds to the molar fraction of the CBZ value equal to $9.6012 \cdot 10^{-4}$. These spectra were measured on a FTIR spectrometer Bruker VERTEX 80v in the wavenumber range of $1000 - 4000 \text{ cm}^{-1}$ with a resolution of 1 cm^{-1} using an HPHT cell [36] with the optical path length $l = 0.118 \text{ cm}$. In order to increase the spectral signal-to-noise ratio, 128 spectra were recorded for each temperature and then they were averaged out. By subtracting the THF spectra weighted by its corresponding mole fraction from the spectra of the CBZ–THF binary mixture, we obtained the CBZ spectrum (Fig. 2a). The C=O spectral region corrected for the base line is presented in (Fig. 2b).

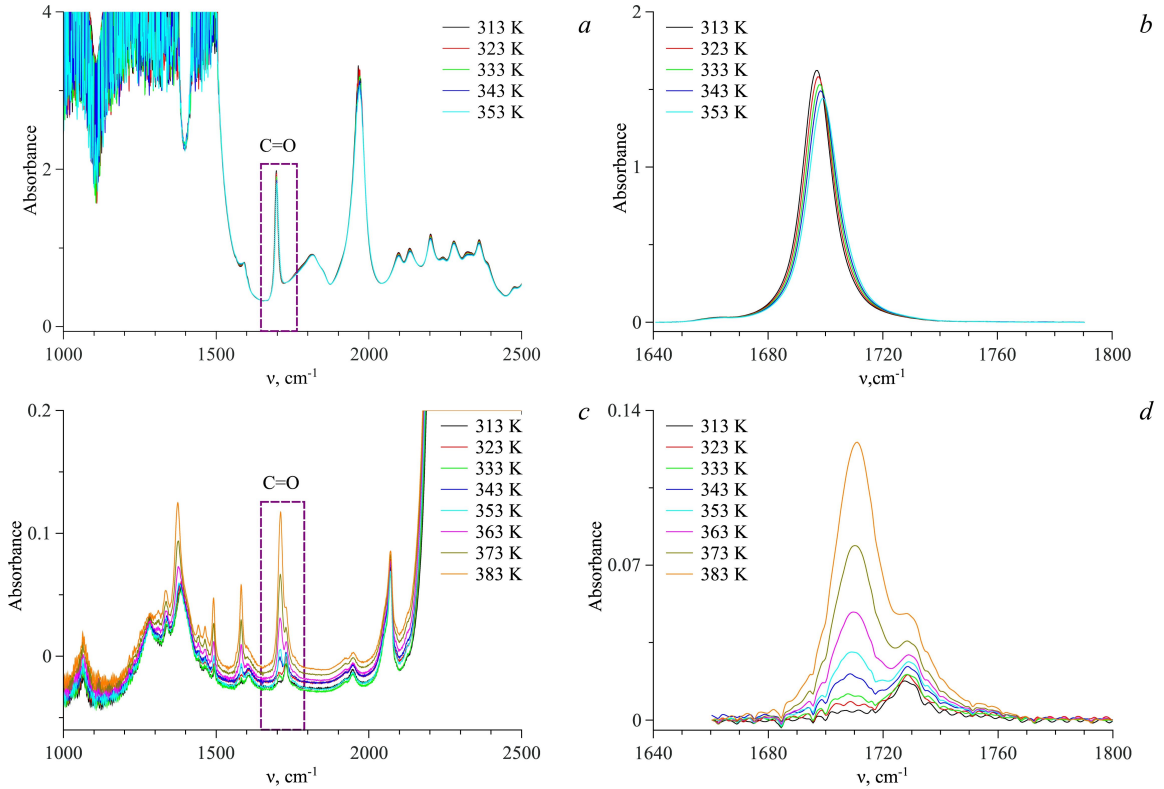


Figure 2: IR spectra of the binary mixtures: CBZ – THF (a), CBZ – scCO_2 (c). The spectral domain bounded by a rectangle corresponds to the analytical spectral band of C=O. The analytical spectral band corrected for the base line contribution for CBZ dissolved in THF (b) and in scCO_2 (d).

In order to estimate the value and the standard deviation of the C=O vibration mode integral intensity for each temperature we measured four spectra with a time interval of 10 minutes. The integral extinction coefficients were averaged for each temperature and the standard deviation was found to be from 0.2% to 0.05% in the whole studied temperature range. As it is shown in Fig. 3, the extinction coefficient is described by a linear equation with a small slope coefficient ($\tan \alpha = -0.253 \text{ km} \cdot \text{mol}^{-1} \cdot \text{K}^{-1}$) at a high accuracy ($R^2 = 0.998$). The linear character of $\varepsilon_{\text{int}} = f(T)$ confirms the absence of specific intermolecular interactions, which was shown in one of our previous works [37].

Within this study, the solubility of CBZ in scCO_2 was measured along two isochores

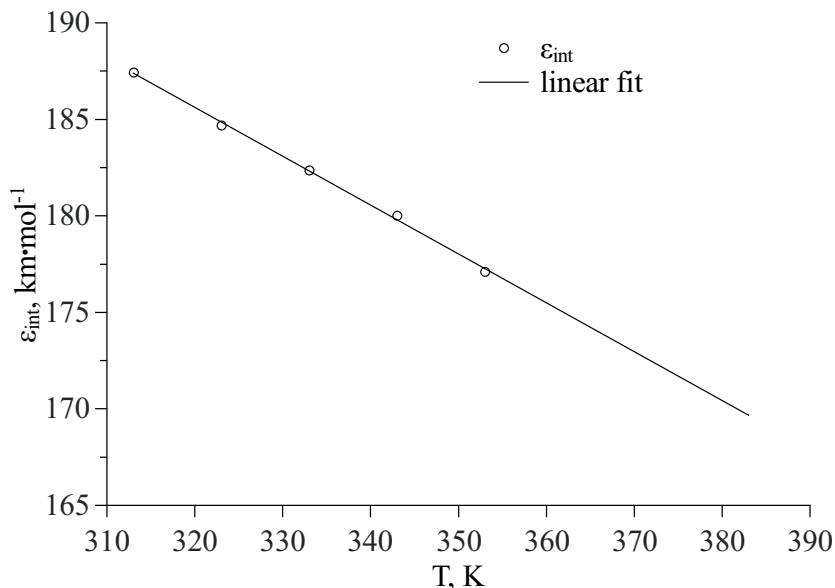


Figure 3: Temperature dependence of integral extinction coefficient and its linear approximation.

corresponding to the density of the fluid phase $\rho = 1.1\rho_{cr}(\text{CO}_2)$ and $\rho = 1.3\rho_{cr}(\text{CO}_2)$ ($\rho_{cr} = 10.6249 \text{ mol/l}$ is the critical density of CO_2) in the temperature range of 313 – 383 K with a step of 10 K. The optical path lengths of the sample for these two measurements were 0.108 cm and 0.097 cm, respectively. The C=O stretching region of the IR spectra of CBZ in sc CO_2 , which were measured in the same way as for the CBZ–THF system, was also analyzed (Fig. 2c,d). These measurements were carried out in a modified high-pressure high-temperature cell described in our work [38]. There was a difference between the shape of the C=O vibration bands in CBZ–THF (Fig. 2a,b) and CBZ–sc CO_2 (Fig. 2c,d) binary systems. In the case of the former system, the C=O vibration mode was symmetric, while in the latter system this band was blue shifted and split into two spectral components, whose intensities and contributions to the total spectral band are sensitive to the temperature increase. We interpret this splitting as a consequence of the presence of two CBZ conformers in the solution. Indeed, in the case of the CBZ–sc CO_2 system, because of the permanent excess of crystalline CBZ being in contact with the solution phase, there was an equilibrium between the CBZ solid phase and its saturated solution in sc CO_2 . As it was shown [39, 40, 38, 41, 42, 43], for drug compounds with different types of polymorphism, there are correlations between the conformers in a solution and polymorphic modifications of their crystalline forms in the bottom phase. Thus, keeping in mind that there is an equilibrium between the solution and the solid phase, one must expect the presence of a conformational equilibrium of the CBZ molecules in the solution. Indeed, the spectral analysis of the C=O vibration mode in the CBZ–sc CO_2 system, carried out based on the results of the quantum chemical calculations, showed that there were two conformers in the solution phase that were responsible for the corresponding spectral contributions to the C=O spectral band. A detailed description of the IR experiment and quantum-chemical calculations was presented in our previous papers [41, 44]. Therefore, the observed splitting of the analytical spectral band for the CBZ–sc CO_2

system is a consequence of the presence of two conformers in the solution.

To calculate the concentration of the CBZ in its saturated solution in scCO₂ we used the value of integral intensity of the C=O vibration band. To obtain this value, we applied a spectral approximation procedure using Fityk software package [45]. Taking into account the results of the quantum chemical calculations we used two spectral profiles to reproduce the analytical spectral band. Therefore, the full integral intensity of the analytical spectral band was calculated as a sum of these components. Then, the solubility of the CBZ dissolved in scCO₂ as a function of temperature was calculated as follows:

$$c_{CBZ}(T) = \frac{A(T)}{l \cdot \varepsilon_{int}(T)}. \quad (14)$$

The molar fraction of CBZ in a scCO₂ solution was calculated according to the equation:

$$X_{CBZ} = \frac{c_{CBZ}}{c_{CBZ} + c_{CO_2}}, \quad (15)$$

where c_{CO_2} is the CO₂ density ($mol \cdot l^{-1}$).

5. Results and discussion

Now we compare the computed and experimental solubility values determined in this paper as well as by Yamini et al. [14]. The comparison is summarized in Fig. 4.

As it was outlined above, our *in situ* IR experiment was conducted under the isochoric conditions, thus, it is rather problematic to make a straightforward comparison. Nevertheless, we show the solubility values corresponding to three temperatures $T = 333\text{ K}$, $T = 343\text{ K}$ and $T = 353\text{ K}$, close to the state parameters, at which the values were obtained by the other methods. It should be outlined that the results of the *in situ* IR experiment correctly represent the solubility behavior within the crossover region, i.e. the inverse dependence of solubility on temperature at a given pressure.

All in all, one can observe qualitative agreement between the obtained results. In addition, it is seen that the trend observed in our previous study of the ibuprofen solubility in scCO₂ [8] is the same, i.e. the solubility values obtained according to the cDFT-based approach are lower than the values from the experiments and MD simulations. This can be correlated with the fact that, as we have already mentioned, this method does not take into account the electrostatic contribution to the solvation free energy of the compound in scCO₂.

It can be seen from the comparison of the solvation free energy values (Fig. 5a) obtained by the cDFT-based approach (dashed lines) and by the MD simulation (symbols) at two temperatures $T = 328\text{ K}$ and $T = 348\text{ K}$. The discrepancies between the values of the solvation free energy correspond to the neglect of the electrostatic contribution within the cDFT approach. In Fig. 5b we demonstrate that the values of the cDFT-calculated solvation free energy are in decent agreement with the values of the Lennard-Jones contribution to the solvation free energy obtained by MD simulation, especially within the crossover region, i.e. at the pressures approximately from 120 to 200 bar.

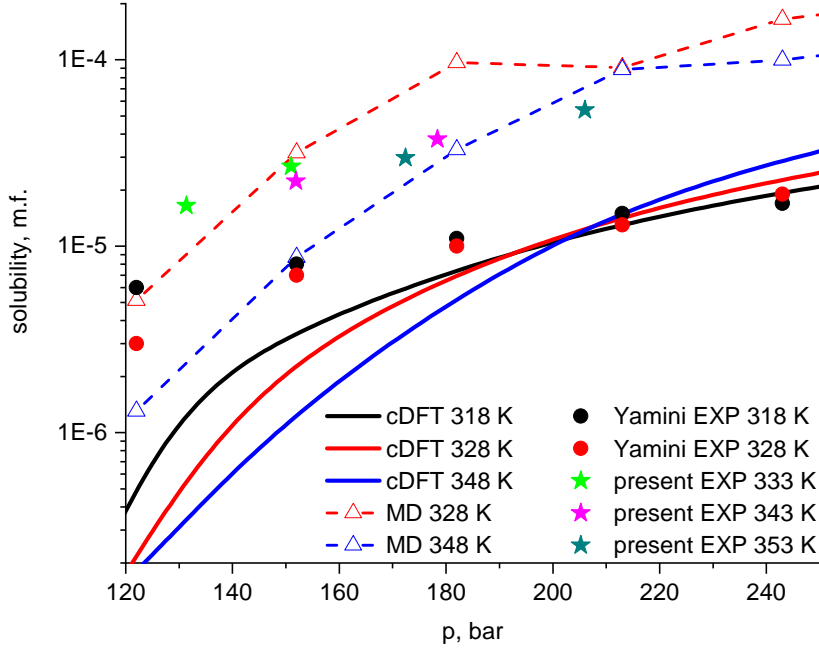


Figure 4: Comparison of the solubility values obtained in accordance with the cDFT approach (solid lines), MD simulation (dashed lines with empty triangles), our *in situ* IR spectroscopy measurements (coloured stars) and the literature data from the experiment by Yamini et al (coloured circles) [14].

Despite the underestimation of the solubility magnitude by the cDFT-based approach, it is important to note that the position of the upper pressure crossover is approximately the same for the cDFT, MD simulation and literature results. The reliable value of the lower pressure crossover for CBZ is hard to determine due to its occurrence in the vicinity of the fluid critical point. Then the cDFT-based approach can be utilized as a preliminary stage, used to narrow the working region for the following experimental procedure [46]. For instance, the estimation of the location of the solubility crossover region can be helpful in the design of extraction processes based on scCO₂ [47].

We compared two isochores, $1.1\rho_{cr}$ and $1.3\rho_{cr}$ obtained from our *in situ* IR measurements with the ones computed in accordance with the cDFT approach. The values of the CBZ concentration in its saturated solution in scCO₂, as obtained from the experimental measurements, are shown in Table 3. In Fig. 6 we show a comparison of the solubility data for these isochores (the coloured symbols are the theoretical results, the empty symbols are the *in situ* IR experiment). As it is expected, the outcomes of the cDFT method underestimate solubility values. The discrepancies in the data are of an order of magnitude for the low temperature range, but the increase in the temperature leads to a decrease in this difference. This is due to the fact that the electrostatics contribution decreases with the temperature increase.

We would also like to discuss the potential limitations and restrictions of the proposed cDFT-based approach. As the input parameters we need to define the critical temperature and pressure of the bioactive compound to obtain the parameters of the LJ interaction potential,

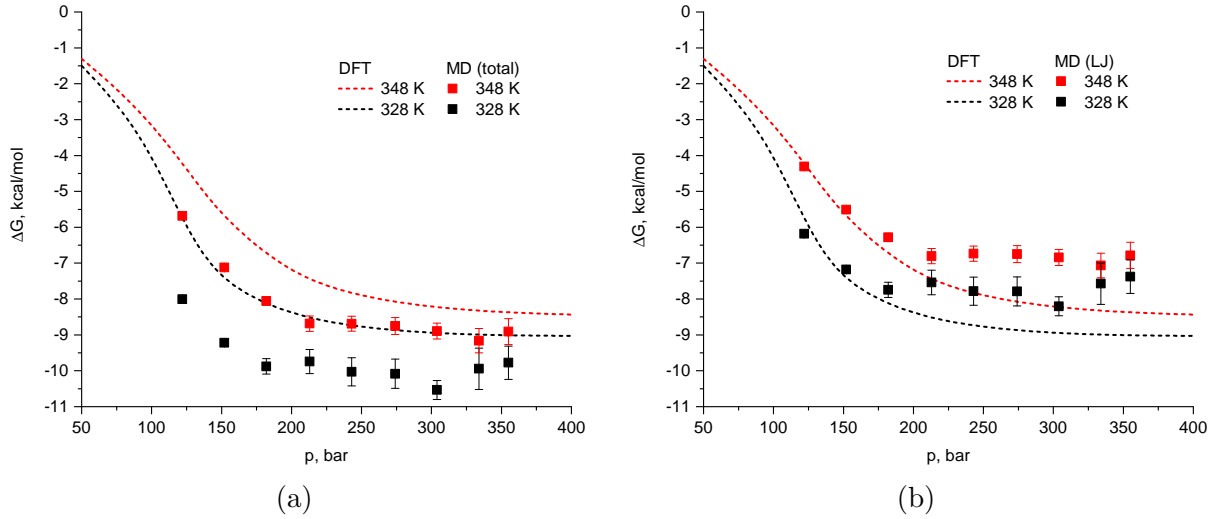


Figure 5: Comparison of the solvation free energy of the compound in scCO_2 obtained from cDFT with the total solvation free energy calculated by MD (a), and with the Lennard-Jones contribution to the solvation free energy calculated by MD (b).

Table 3: The temperature dependence of the CBZ concentration in the saturated solution in scCO_2 and its molar fraction in scCO_2 for two isochores.

T, K	Isochore 1.1			Isochore 1.3		
	p, bar	$c \cdot 10^4, \text{mol} \cdot \text{l}^{-1}$	$X \cdot 10^5, m.f.$	p, bar	$c \cdot 10^4, \text{mol} \cdot \text{l}^{-1}$	$X \cdot 10^5, m.f.$
313				97.54	2.36	1.71
323				124.00	2.94	2.13
333	131.43	1.93	1.65	151.02	3.71	2.68
343	151.89	2.61	2.23	178.41	5.19	3.76
353	172.43	3.48	2.98	206.02	7.43	5.37
363	193.02	4.96	4.25	233.76	10.75	7.78
373	213.63	7.33	6.27	261.56	16.39	11.87
383	234.25	11.09	9.49	298.41	25.43	18.41

and also find the data for the sublimation pressure and molar volume of the compound, as it was discussed above. Such task may have some pitfalls. It is clear that the critical parameters for the API molecule can be determined only through some approximations. In our case the values of the critical parameters for CBZ taken from the literature were calculated within the Group Contribution Method [48]. In short, such method relates, in a certain way, the thermodynamic properties of a compound with its molecular structure. The thing is that there are a number of such correlations, which can in the end lead to a drastic divergence, with CBZ being no exception. For example, the value of the critical temperature is $1197.01 K$ (Kikic et al [49]) and $786.83 K$ (Li et al [21]). In principle, one can try to fit the experimental data of solubility using the potential parameters, but in this case cDFT would fail to estimate the position of the crossover points. We believe that the possibility

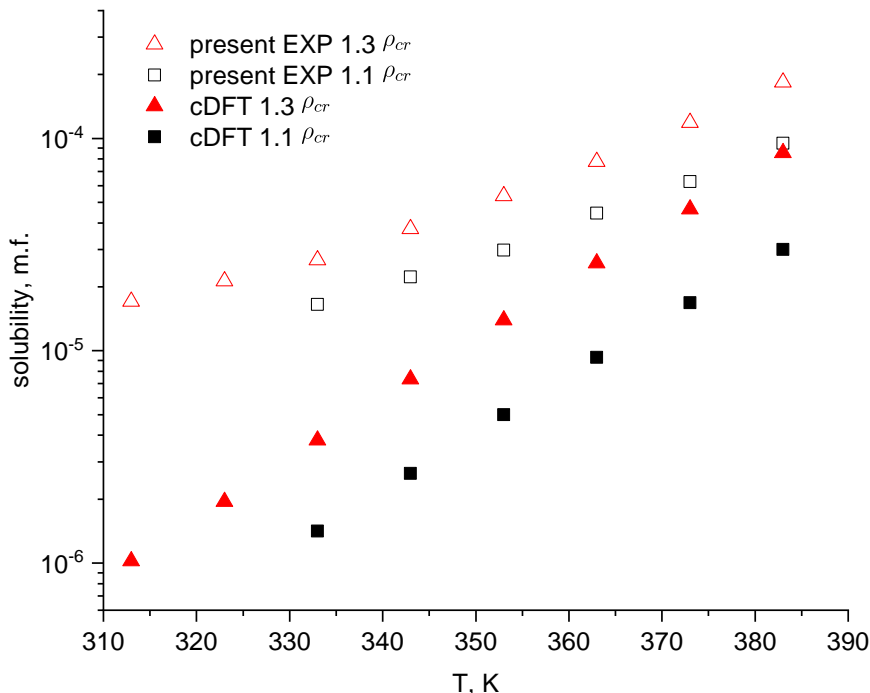


Figure 6: Comparison of the solubility values for two isochores $1.1\rho_{cr}$ and $1.3\rho_{cr}$ for CBZ in scCO_2 obtained from the cDFT and our *in situ* IR measurements.

of correct estimation of the pressure crossover is crucial for further applications. Thus, one has to bear in mind that inaccurate estimation of the compound critical parameters can lead to incorrect results. Another problem is the accurate determination of the sublimation pressure values and molar volume of the compound as they also play a crucial role in the determination of the solubility values. Again, approximate methods do not always seem to produce decent results [21], as compared with the strict experiment [22].

6. Conclusions and prospects

We have obtained values of CBZ solubility in scCO_2 using the experimental *in situ* IR approach, MD simulation and theoretical computation. All the obtained results were also compared with the experimental data available in literature.

We have measured two solubility isochores corresponding to the density of $1.1\rho_{cr}$ and $1.3\rho_{cr}$ via the *in situ* IR spectroscopy, where the extinction coefficient of the C=O vibration was first determined in a mixture of CBZ and THF at infinite dilution and at different temperatures in the range between 313 K and 353 K. This allows an accurate determination of the solubility using the Beer-Lambert law. We have computed the solvation free energy of CBZ in scCO_2 within the MD simulation for two isotherms: 328 K and 348 K, and calculated the solubility based on these results. The same isochores and isotherms were computed according to the theoretical cDFT-based approach. The results of the latter are in qualitative agreement with the experiment and simulation, and, despite the neglect of the

electrostatic solute-solvent interactions, they reproduce the position of the upper pressure crossover with reasonable accuracy.

In conclusion, we would like to speculate on the possible applications of our cDFT-based approach. Firstly, this approach could be utilized for predicting the pressure crossover region within the region of the active compound solubility in scCO₂ provided that the sublimation pressure and the critical parameters for the solute are available. In addition, this approach can be implemented as a software tool in a possible complex experimental setup of solubility data treatment along with the *in situ* IR-based methodology presented above.

7. Acknowledgements

The research was supported by the Russian Federal Program (grant no. RFMEFI61618×0097). The IR spectroscopy experiment was performed using the molecular fluid spectroscopy facility (<http://www.ckp-rf.ru/usu/503933/>) of G.A. Krestov Institute of Solution Chemistry of the Russian Academy of Sciences (ISC RAS) (Russia). MD simulations were performed using the supercomputer facilities provided by NRU HSE.

References

- [1] L. Padrela, M. A. Rodrigues, A. Duarte, A. M. Dias, M. E. Braga, and H. C. de Sousa, "Supercritical carbon dioxide-based technologies for the production of drug nanoparticles/nanocrystals—a comprehensive review," *Advanced drug delivery reviews*, vol. 131, pp. 22–78, 2018.
- [2] L. X. Yu, G. L. Amidon, J. E. Polli, H. Zhao, M. U. Mehta, D. P. Conner, V. P. Shah, L. J. Lesko, M.-L. Chen, V. H. Lee, *et al.*, "Biopharmaceutics classification system: the scientific basis for biowaiver extensions," *Pharmaceutical research*, vol. 19, no. 7, pp. 921–925, 2002.
- [3] V. P. Shah and G. L. Amidon, "GL Amidon, H Lennernas, VP Shah, and JR Crison. a theoretical basis for a biopharmaceutic drug classification: The correlation of in vitro drug product dissolution and in vivo bioavailability, pharm res 12, 413–420, 1995—backstory of bcs," *The AAPS journal*, vol. 16, no. 5, pp. 894–898, 2014.
- [4] A. M. Healy, Z. A. Worku, D. Kumar, and A. M. Madi, "Pharmaceutical solvates, hydrates and amorphous forms: A special emphasis on cocrystals," *Advanced drug delivery reviews*, vol. 117, pp. 25–46, 2017.
- [5] D. D. Bavishi and C. H. Borkhataria, "Spring and parachute: How cocrystals enhance solubility," *Progress in Crystal Growth and Characterization of Materials*, vol. 62, no. 3, pp. 1–8, 2016.
- [6] A. T. Serajuddin, "Salt formation to improve drug solubility," *Advanced drug delivery reviews*, vol. 59, no. 7, pp. 603–616, 2007.
- [7] P. Kanaujia, P. Poovizhi, W. Ng, and R. Tan, "Amorphous formulations for dissolution and bioavailability enhancement of poorly soluble apis," *Powder technology*, vol. 285, pp. 2–15, 2015.
- [8] Y. Budkov, A. Kolesnikov, D. Ivlev, N. Kalikin, and M. Kiselev, "Possibility of pressure crossover prediction by classical dft for sparingly dissolved compounds in scCO₂," *Journal of Molecular Liquids*, vol. 276, pp. 801–805, 2019.
- [9] R. J. Schain, J. W. Ward, and D. Guthrie, "Carbamazepine as an anticonvulsant in children," *Neurology*, vol. 27, no. 5, pp. 476–476, 1977.
- [10] P. Wiffen, H. McQuay, and R. Moore, "Carbamazepine for acute and chronic pain.," 2005.
- [11] R. A. Kowatch, T. Suppes, T. J. Carmody, J. P. Bucci, J. H. Hume, M. Kromelis, G. J. Emslie, W. A. Weinberg, and A. J. Rush, "Effect size of lithium, divalproex sodium, and carbamazepine in children and adolescents with bipolar disorder," *Journal of the American Academy of Child & Adolescent Psychiatry*, vol. 39, no. 6, pp. 713–720, 2000.
- [12] W. H. Organization *et al.*, "The selection and use of essential medicines: report of the who expert committee, 2013 (including the 18th who model list of essential medicines and the 4th who model list of essential medicines for children)," tech. rep., World Health Organization, 2014.
- [13] P. Zakeri-Milani, M. Barzegar-Jalali, M. Azimi, and H. Valizadeh, "Biopharmaceutical classification of drugs using intrinsic dissolution rate (idr) and rat intestinal permeability," *European journal of pharmaceuticals and biopharmaceutics*, vol. 73, no. 1, pp. 102–106, 2009.
- [14] Y. Yamini, J. Hassan, and S. Haghgo, "Solubilities of some nitrogen-containing drugs in supercritical carbon dioxide," *Journal of Chemical & Engineering Data*, vol. 46, no. 2, pp. 451–455, 2001.
- [15] J. Noroozi, C. Ghotbi, J. J. Sardroodi, J. Karimi-Sabet, and M. A. Robert, "Solvation free energy and solubility of acetaminophen and ibuprofen in supercritical carbon dioxide: Impact of the solvent model," *The Journal of Supercritical Fluids*, vol. 109, pp. 166–176, 2016.
- [16] H. C. Andersen, J. D. Weeks, and D. Chandler, "Relationship between the hard-sphere fluid and fluids with realistic repulsive forces," *Physical Review A*, vol. 4, no. 4, p. 1597, 1971.
- [17] Y. Rosenfeld, "Free-energy model for the inhomogeneous hard-sphere fluid mixture and density-functional theory of freezing," *Physical review letters*, vol. 63, no. 9, p. 980, 1989.
- [18] R. Roth, "Fundamental measure theory for hard-sphere mixtures: a review," *Journal of Physics: Condensed Matter*, vol. 22, no. 6, p. 063102, 2010.
- [19] L. Verlet and J.-J. Weis, "Equilibrium theory of simple liquids," *Physical Review A*, vol. 5, no. 2, p. 939, 1972.
- [20] E. W. Lemmon, M. O. McLinden, and D. G. Friend, *Thermophysical properties of fluid systems*. NIST chemistry WebBook, 1998.

- [21] J.-h. Li, Z. Huang, J.-l. Wei, and L. Xu, "A new optimization method for parameter determination in modeling solid solubility in supercritical co₂," *Fluid Phase Equilibria*, vol. 344, pp. 117–124, 2013.
- [22] K. V. Drozd, A. N. Manin, A. V. Churakov, and G. L. Perlovich, "Novel drug–drug cocrystals of carbamazepine with para-aminosalicylic acid: Screening, crystal structures and comparative study of carbamazepine cocrystal formation thermodynamics," *CrystEngComm*, vol. 19, no. 30, pp. 4273–4286, 2017.
- [23] C. H. Bennett, "Efficient estimation of free energy differences from monte carlo data," *Journal of Computational Physics*, vol. 22, no. 2, pp. 245–268, 1976.
- [24] M. R. Shirts and V. S. Pande, "Comparison of efficiency and bias of free energies computed by exponential averaging, the bennett acceptance ratio, and thermodynamic integration," *The Journal of chemical physics*, vol. 122, no. 14, p. 144107, 2005.
- [25] M. R. Shirts and V. S. Pande, "Solvation free energies of amino acid side chain analogs for common molecular mechanics water models," *The Journal of chemical physics*, vol. 122, no. 13, p. 134508, 2005.
- [26] A. I. Frolov, "Accurate calculation of solvation free energies in supercritical fluids by fully atomistic simulations: Probing the theory of solutions in energy representation," *Journal of chemical theory and computation*, vol. 11, no. 5, pp. 2245–2256, 2015.
- [27] B. Hess, C. Kutzner, D. Van Der Spoel, and E. Lindahl, "Gromacs 4: algorithms for highly efficient, load-balanced, and scalable molecular simulation," *Journal of chemical theory and computation*, vol. 4, no. 3, pp. 435–447, 2008.
- [28] A. K. Malde, L. Zuo, M. Breeze, M. Stroet, D. Poger, P. C. Nair, C. Oostenbrink, and A. E. Mark, "An automated force field topology builder (atb) and repository: version 1.0," *Journal of chemical theory and computation*, vol. 7, no. 12, pp. 4026–4037, 2011.
- [29] N. Schmid, A. P. Eichenberger, A. Choutko, S. Riniker, M. Winger, A. E. Mark, and W. F. van Gunsteren, "Definition and testing of the gromos force-field versions 54a7 and 54b7," *European biophysics journal*, vol. 40, no. 7, p. 843, 2011.
- [30] U. C. Singh and P. A. Kollman, "An approach to computing electrostatic charges for molecules," *Journal of Computational Chemistry*, vol. 5, no. 2, pp. 129–145, 1984.
- [31] B. H. Besler, K. M. Merz Jr, and P. A. Kollman, "Atomic charges derived from semiempirical methods," *Journal of Computational Chemistry*, vol. 11, no. 4, pp. 431–439, 1990.
- [32] M. Frisch, G. Trucks, H. Schlegel, G. Scuseria, M. Robb, J. Cheeseman, G. Scalmani, V. Barone, B. Mennucci, G. Petersson, *et al.*, "Gaussian 09, revision b. 01; wallingford, ct, 2009," 2013.
- [33] Z. Zhang and Z. Duan, "An optimized molecular potential for carbon dioxide," *The Journal of chemical physics*, vol. 122, no. 21, p. 214507, 2005.
- [34] H. Paliwal and M. R. Shirts, "A benchmark test set for alchemical free energy transformations and its use to quantify error in common free energy methods," *Journal of chemical theory and computation*, vol. 7, no. 12, pp. 4115–4134, 2011.
- [35] R. Oparin, E. Vorobyev, and M. Kiselev, "A new method for measuring the solubility of slightly soluble substances in supercritical carbon dioxide," *Russian Journal of Physical Chemistry B*, vol. 10, no. 7, pp. 1108–1115, 2016.
- [36] R. D. Oparin, A. Idrissi, M. V. Fedorov, and M. G. Kiselev, "Dynamic and static characteristics of drug dissolution in supercritical co₂ by infrared spectroscopy: measurements of acetaminophen solubility in a wide range of state parameters," *Journal of Chemical & Engineering Data*, vol. 59, no. 11, pp. 3517–3523, 2014.
- [37] R. Oparin, T. Tassaing, Y. Danten, and M. Besnard, "Water-carbon dioxide mixtures at high temperatures and pressures: Local order in the water rich phase investigated by vibrational spectroscopy," *The Journal of chemical physics*, vol. 123, no. 22, p. 224501, 2005.
- [38] R. D. Oparin, Y. A. Vaksler, M. A. Krestyaninov, A. Idrissi, S. V. Shishkina, and M. G. Kiselev, "Polymorphism and conformations of mefenamic acid in supercritical carbon dioxide," *The Journal of Supercritical Fluids*, p. 104547, 2019.
- [39] R. D. Oparin, M. Moreau, I. De Walle, M. Paolantoni, A. Idrissi, and M. G. Kiselev, "The interplay between the paracetamol polymorphism and its molecular structures dissolved in supercritical co₂ in

- contact with the solid phase: In situ vibration spectroscopy and molecular dynamics simulation analysis,” *European Journal of Pharmaceutical Sciences*, vol. 77, pp. 48–59, 2015.
- [40] R. Oparin, D. Ivlev, A. Vorobei, A. Idrissi, and M. Kiselev, “Screening of conformational polymorphism of ibuprofen in supercritical co₂,” *Journal of Molecular Liquids*, vol. 239, pp. 49–60, 2017.
 - [41] R. Oparin, D. Ivlev, and M. Kiselev, “Conformational equilibria of pharmaceuticals in supercritical co₂, ir spectroscopy and quantum chemical calculations,” *Spectrochimica Acta Part A: Molecular and Biomolecular Spectroscopy*, p. 118072, 2020.
 - [42] I. Khodov, S. Efimov, V. Klochkov, G. Alper, and L. B. De Carvalho, “Determination of preferred conformations of ibuprofen in chloroform by 2d noe spectroscopy,” *European Journal of Pharmaceutical Sciences*, vol. 65, pp. 65–73, 2014.
 - [43] I. A. Khodov, S. V. Efimov, M. Y. Nikiforov, V. V. Klochkov, and N. Georgi, “Inversion of population distribution of felodipine conformations at increased concentration in dimethyl sulfoxide is a prerequisite to crystal nucleation,” *Journal of pharmaceutical sciences*, vol. 103, no. 2, pp. 392–394, 2014.
 - [44] R. D. Oparin, M. V. Kurskaya, M. A. Krestyaninov, A. Idrissi, and M. G. Kiselev, “Correlation between the conformational crossover of carbamazepine and its polymorphic transition in supercritical co₂: On the way to polymorph control,” *European Journal of Pharmaceutical Sciences*, p. 105273, 2020.
 - [45] M. Wojdyr, “Fityk: a general-purpose peak fitting program,” *Journal of Applied Crystallography*, vol. 43, no. 5-1, pp. 1126–1128, 2010.
 - [46] N. R. Foster, G. S. Gurdial, J. S. Yun, K. K. Liong, K. D. Tilly, S. S. Ting, H. Singh, and J. H. Lee, “Significance of the crossover pressure in solid-supercritical fluid phase equilibria,” *Industrial & engineering chemistry research*, vol. 30, no. 8, pp. 1955–1964, 1991.
 - [47] J. F. Brennecke and C. A. Eckert, “Phase equilibria for supercritical fluid process design,” *AIChE Journal*, vol. 35, no. 9, pp. 1409–1427, 1989.
 - [48] K. Klinecicz and R. Reid, “Estimation of critical properties with group contribution methods,” *AIChE Journal*, vol. 30, no. 1, pp. 137–142, 1984.
 - [49] I. Kikic, N. De Zordi, M. Moneghini, and D. Solinas, “Solubility estimation of drugs in ternary systems of interest for the antisolvent precipitation processes,” *The Journal of Supercritical Fluids*, vol. 55, no. 2, pp. 616–622, 2010.